JOURNAL OF GUIDANCE, CONTROL, AND DYNAMICS
Vol. 32, No. 2, March–April 2009

# Use of Pitch and Heave Motion Cues in a Pitch Control Task

P. M. T. Zaal,* D. M. Pool,† J. de Bruin,‡ M. Mulder,§ and M. M. van Paassen¶
*Delft University of Technology, 2600 GB Delft, The Netherlands*

DOI: 10.2514/1.39953

**During pitch rotation of the aircraft, a pilot, seated in front of the aircraft center of gravity, is subjected to rotational pitch and vertical heave motion. The heave motion is a combination of the vertical motion of the aircraft center of gravity and the heave motion as a result of the pitch rotation. In a pitch tracking task, all of these cues could potentially have a positive effect on performance and control behavior, as they are all related to the aircraft pitch attitude. To improve the tuning of flight simulator motion filters, a better understanding of how these motion components are used by the pilot is required. First, the optimal use of the different motion components was evaluated using an optimal control analysis. Next, an aircraft pitch attitude control experiment was performed in the SIMONA Research Simulator, investigating the effects of pitch rotation, pitch heave, and center of gravity heave on pilot control behavior. Pilot performance significantly improved with pitch motion, with an increased crossover frequency for the disturbance open loop. The increase in performance was a result of an increased visual gain and a reduction in visual lead, allowed for by the addition of pitch motion. Pitch heave motion showed similar but smaller effects. The center of gravity heave motion, although taking up most of the simulator motion space, was found to have no significant effects on performance and control behavior.**

## Nomenclature

| | | |
|---|---|---|
| $A$ | = | sinusoid amplitude, deg |
| $a_z$ | = | heave acceleration, m · s$^{-2}$ |
| $e$ | = | tracking error signal, rad |
| $F$ | = | feedback gain |
| $f$ | = | forcing function signal, rad |
| $f_d$ | = | disturbance forcing function, rad |
| $f_t$ | = | target forcing function, rad |
| $H(j\omega)$ | = | frequency response function |
| $H(s)$ | = | transfer function |
| $J$ | = | criterion function, rad$^2$ |
| $K_m$ | = | motion perception gain |
| $K_v$ | = | visual perception gain |
| $l$ | = | distance between the center of gravity and pilot station, m |
| $N$ | = | number of points |
| $n$ | = | pilot remnant signal, rad |
| $n_d$ | = | disturbance forcing function frequency integer factor |
| $n_t$ | = | target forcing function frequency integer factor |
| $Q$ | = | optimal control performance gain |
| $R$ | = | optimal control effort gain |
| $s$ | = | Laplace variable |
| $T_{\text{lead}}$ | = | visual lead time constant, s |
| $T_{\text{lag}}$ | = | visual lag time constant, s |
| $T_m$ | = | measurement time, s |
| $t$ | = | time, s |
| $u$ | = | pilot control signal, rad |
| $z$ | = | vertical displacement, m |
| $\delta_e$ | = | elevator deflection, rad |
| $\zeta_{nm}$ | = | neuromuscular damping |
| $\theta$ | = | pitch angle, rad |
| $\dot{\theta}$ | = | pitch rate, rad · s$^{-1}$ |
| $\ddot{\theta}$ | = | pitch acceleration, rad · s$^{-2}$ |
| $\sigma$ | = | standard deviation |
| $\tau_m$ | = | motion perception time delay, s |
| $\tau_v$ | = | visual perception time delay, s |
| $\phi$ | = | sinusoid phase shift, rad |
| $\varphi_m$ | = | phase margin, deg |
| $\omega$ | = | frequency, rad · s$^{-1}$ |
| $\omega_c$ | = | crossover frequency, rad · s$^{-1}$ |
| $\omega_{nm}$ | = | neuromuscular frequency, rad · s$^{-1}$ |

*Subscripts*

| | | |
|---|---|---|
| $d$ | = | disturbance |
| $t$ | = | target |

Presented as Paper 6537 at the AIAA Modeling and Simulation Technologies Conference and Exhibit, Honolulu, HI, 18–21 August 2008; received 22 July 2008; revision received 3 October 2008; accepted for publication 10 October 2008. 

*Ph.D. Candidate, Control and Simulation Division, Faculty of Aerospace Engineering, P.O. Box 5058; p.m.t.zaal@tudelft.nl. Student member AIAA.

†Ph.D. Candidate, Control and Simulation Division, Faculty of Aerospace Engineering, P.O. Box 5058; d.m.pool@tudelft.nl. Student member AIAA.

‡M.Sc. Student, Control and Simulation Division, Faculty of Aerospace Engineering, P.O. Box 5058; debruin.jaap@gmail.com.

§Associate Professor, Control and Simulation Division, Faculty of Aerospace Engineering, P.O. Box 5058; m.mulder@tudelft.nl. Member AIAA.

¶Associate Professor, Control and Simulation Division, Faculty of Aerospace Engineering, P.O. Box 5058; m.m.vanpaassen@tudelft.nl. Member AIAA.

## I. Introduction

MANY studies in the last decades have focused on the effects of motion cues on pilot performance and control behavior in manual piloting tasks that occur in aviation. Most of these studies focused on manual control of one of the aircraft rotational degrees of freedom. A significant body of literature is available on the influence of motion cues in the control of aircraft roll attitude [1–4], yaw attitude [5–8], and pitch attitude [9–11]. In actual aircraft, however, rotational motion rarely occurs without some coupled translational motion. For instance, normal aircraft roll maneuvers are *coordinated*, which means that the linear lateral motion of the aircraft will clearly influence the overall sensation of motion. This study focuses on pitch attitude control, during which a similar coupling between rotational and vertical motion is present.

Pitch rotation in a conventional aircraft with the pilot seated in front of the center of aircraft body rotation will result in three components of motion at the pilot station: 1) rotational pitch motion (PM), 2) vertical (heave) motion directly due to pitch rotation and dependent on the distance from the pilot station to the center of rotation, and 3) vertical motion of the aircraft center of gravity that results from the pitch rotation. These distinctly different contributions to the total perceived physical motion at the pilot

station may all affect the pilot's control of pitch attitude. This warrants a study similar to the recent research effort that investigated the relative importance of yaw and sway motion cues in lateral helicopter control [6–8].

Only a few studies described in the literature investigate the influence of vertical motion on pitch control [10,11]. Steurs et al. [10] compared the results of a simulator experiment with those of an in-flight experiment performed in a Cessna Citation II. In the simulator experiment, a nonlinear Cessna Citation model was controlled for systematically varying pitch and heave motion settings. The total vertical motion as perceived at the pilot station, filtered by a washout filter, was used as the heave acceleration in the simulator experiment. No distinction was made between the two types of heave motion cues described. This study showed a positive effect of pitch motion on pilot tracking performance and a smaller positive effect of heave motion.

Dehouck et al. [11] performed an experiment to investigate the effect of motion filter settings on a pitch tracking and disturbance-rejection task of a system with double integrator dynamics. The presence of pitch motion was found to improve the pilots' performance and increase their control bandwidth. As a secondary research goal, the influence of heave motion, chosen to be proportional to the pitch acceleration, was investigated. A significant increase in performance was found when this type of heave motion was present. In this study, heave motion was presented only in trials in which pitch motion was also available.

Hence, the individual and combined effects of pitch and heave motion on pilot control behavior in an aircraft pitch control task remain largely unclear. This study aims to increase the insight into the possible effects of the different pitch and heave motion cues during aircraft pitching motion. As pitch control is also the planned subject of future in-flight experiments [12] that will be performed in Delft University of Technology's Citation II laboratory aircraft, a pitch control task is considered that is representative for this aircraft.

The paper is structured as follows. First, the pitch attitude control task and the motion cues that are important during pitching maneuvers are introduced. Then, the relative importance of the feedback of pitch attitude and its derivatives for increasing the performance of a closed-loop pitch attitude control system is investigated using an optimal control analysis. The remainder of this paper describes the setup and results of a human-in-the-loop experiment in which the effects of pitch and heave motion cues on pitch attitude control behavior were evaluated.

## II. Pitch Attitude Control Task

In conventional fixed-wing aircraft, the pilot station is generally located in front of the aircraft center of gravity. The motion that pilots are subjected to during flight are a superposition of movement of the aircraft center of gravity, rigid body rotation around the aircraft center of gravity, and possible aeroelastic effects [13]. A clear example of this is a pitch maneuver, that is, a change in aircraft pitch attitude, of which a schematic representation is depicted in Fig. 1.

Figure 1 illustrates that, during changes in pitch attitude $\theta$, vertical motion will also be present at the pilot station, in addition to the obvious pitch rotation. For instance, a change in pitch attitude will cause a change in aircraft altitude, yielding relatively low-frequency vertical (heave) motion of the aircraft center of gravity. This component of the symmetrical aircraft motion will be referred to as "c.g. heave" in this study, indicated by $a_{z_{cg}}$ in Fig. 1. In addition, the pitch rotation around the aircraft c.g. directly induces extra heave motion at the pilot station, due to the position of the pilot station with respect to the aircraft c.g.. This latter heave component will be referred to as "pitch heave" (PH) in this study and is denoted by $a_{z_\theta}$. Using the definitions and conventions shown in Fig. 1, the total heave acceleration at the pilot station during pitch maneuvers can be denoted as follows:

$$a_z = a_{z_{cg}} + a_{z_\theta} = a_{z_{cg}} - l\ddot{\theta} \tag{1}$$

In Eq. (1), $l$ is the distance in longitudinal direction between the aircraft c.g. and the pilot station; $\ddot{\theta}$ denotes the pitch acceleration. Note that, despite the fact that there may be an additional small vertical offset between the aircraft c.g. and pilot station, only the effects of the longitudinal offset $l$ are considered here.

The greater the distance $l$ between the pilot station and center of gravity, that is, the larger the aircraft under consideration, the more dominant the pitch heave component $a_{z_\theta}$ will be. Some argue that for certain types of aircraft the linear motion cues that result from changes in the aircraft attitude even dominate pilots' perception of rotational motion [6]. To evaluate the relative importance of the different types of motion cues during changes in aircraft pitch attitude, their effects on the closed-loop manual control of aircraft pitch will be investigated in this study. More specifically, the effects of aircraft pitch and heave motion cues in a manual pitch attitude control task, as depicted in Fig. 2, will be studied.

The basis for this study will be the compensatory tracking task, considered in many previous studies on human manual control behavior [2,3,14] for aircraft pitch, $\theta$. In such a compensatory tracking task, the pilot's objective is to actively minimize the deviation from the desired aircraft state, that is, the tracking error, denoted by $e$ in Fig. 2, which is depicted on a visual display. The compensatory tracking task studied in this paper is a disturbance-rejection task, where the pilot is required to counteract the influence of a disturbance signal. This disturbance signal is indicated with the symbol $f_d$ in Fig. 2. In addition to this disturbance signal, an independent target signal $f_t$ is also introduced into the closed-loop system (see Fig. 2), which represents the commanded pitch attitude. This second signal, which was designed with a significantly reduced magnitude compared with $f_d$, serves the purpose to allow for identification of both visual and motion responses for this task [15].

During compensatory pitch control in an aircraft, pilots receive additional feedback of aircraft pitch and heave motion, as indicated in Fig. 2. This allows pilots to close extra stabilizing feedback loops around the controlled aircraft dynamics, as both pitch and heave motion cues are correlated with aircraft pitch.

Anticipating future in-flight experiments that are to be performed with the Delft University of Technology Cessna Citation II laboratory aircraft, the vehicle dynamics that are used throughout this study are those of the Cessna Citation I Ce500 [16]. For this aircraft, the distance $l$ of the pilot station to the center of gravity is 3.2 m. This is relatively small compared with large transport aircraft, which have typical distances on the order of 15–20 m. In this study, a reduced linear model of the aircraft is used, trimmed at an altitude of 10,000 ft (3048 m) and at an airspeed of 160 kt (87 m/s). The controlled aircraft pitch dynamics, relating elevator input $\delta_e$ to aircraft pitch attitude $\theta$, are given by Eq. (2):

$$H_{\theta,\delta_e}(s) = -10.6189\frac{s + 0.9906}{s(s^2 + 2.756s + 7.612)} \tag{2}$$

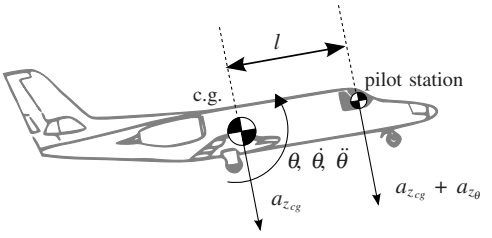


**Fig. 1 Aircraft motion at the center of gravity and pilot station during a pitch maneuver.**

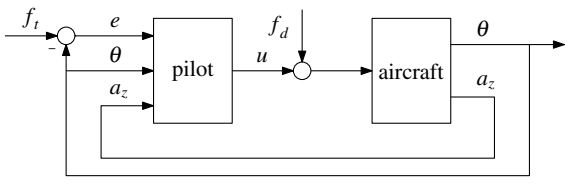


**Fig. 2 Schematic representation of a closed-loop compensatory aircraft pitch control task.**

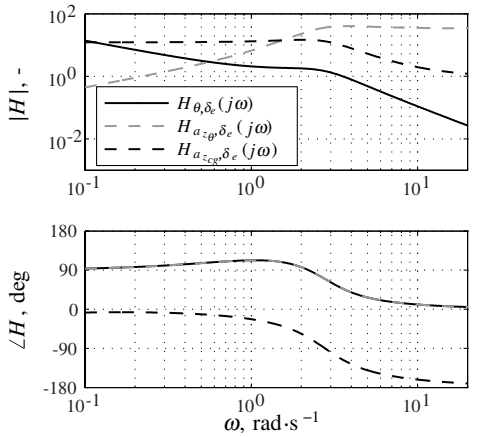


**Fig. 3 Bode magnitude and phase of relevant aircraft model elevator responses.**

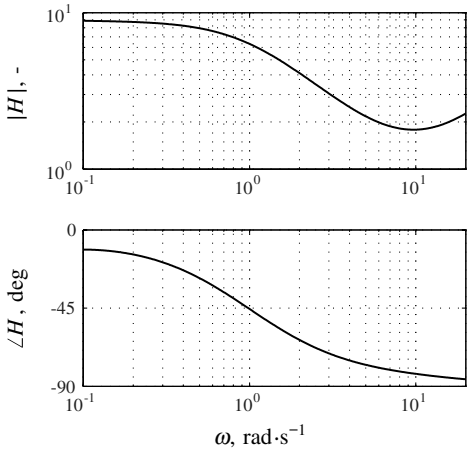


**Fig. 4 Bode magnitude and phase of the transfer function that relates negative pitch rate $-\theta$ to c.g. heave $a_{z_{cg}}$.**

$$H_{\theta,a_{z_{cg}}}(s) = -0.97202\frac{(s-10.08)(s+9.536)(s+0.009785)}{s(s^2+2.756s+7.612)} \tag{3}$$

The transfer function for the heave acceleration at the pilot station due to the pitch rotation, $a_{z_\theta}$, can be easily deduced from Eqs. (1) and (2). The c.g. heave acceleration $a_{z_{cg}}$, which is a result of a slower altitude mode of the aircraft dynamics, has a less direct relation to the pitch dynamics $H_{\theta,\delta_e}(s)$ and is defined by Eq. (3). A Bode graph of the aircraft model pitch dynamics and both heave motion components is depicted in Fig. 3. The fact that the Bode phases of $H_{\theta,\delta_e}(j\omega)$ and $H_{a_{z_\theta},\delta_e}(j\omega)$ coincide is caused by the fact that $a_{z_\theta} = -l\ddot{\theta}$. This implies that there is a double differentiation *and* a minus sign between the responses of $\theta$ and $a_{z_\theta}$ to an elevator command, yielding a total shift in phase of 360 (or 0) deg.

For the pitch attitude control task that is studied here, $H_{\theta,\delta_e}(j\omega)$ defines the controlled element dynamics, depicted in Fig. 3 as solid black lines. For the lower frequencies, up to approximately 0.8 rad/s, the pitch dynamics are a single integrator. Then, up to the peak that results from the short period eigenmode at approximately 2.5 rad/s, the Citation pitch dynamics are a gain. Finally, for frequencies above the eigenfrequency of the short period mode, the system behaves like a double integrator.

A comparison of the Bode magnitude of both the pitch heave and c.g. heave components in Fig. 3 reveals that the pitch heave acceleration $a_{z_\theta}$ is a high-pass signal, with most of its power at the higher frequencies. For $a_{z_{cg}}$ during pitch maneuvers the opposite holds: c.g. heave is a low-pass response to an elevator deflection $\delta_e$. The relatively high low-frequency power of the c.g. heave corresponds to the slow, large-amplitude motions that occur during changes in aircraft altitude (climb or descent). To illustrate the relation between c.g. heave and pitch attitude and its derivatives, Fig. 4 shows a Bode graph of the transfer function from negative pitch rate to c.g. heave: $H_{a_{z_{cg}},-\dot{\theta}} = H_{a_{z_{cg}},\delta_e}/(-H_{\dot{\theta},\delta_e})$. Note from Fig. 4 that, for low frequencies of up to 0.6 rad/s, c.g. heave is more or less proportional to pitch rate $\dot{\theta}$, whereas for higher frequencies it is more related to pitch attitude $\theta$. The c.g. heave motion has the least straightforward relation with the controlled pitch attitude, meaning that its usefulness for manual pitch control is questionable.

Note from the corresponding phase responses in Fig. 3 that, for the higher frequencies, there is a 180 deg phase difference between the two heave components, which implies that during aircraft pitch rotation both heave motion components partially cancel each other.

To summarize, the three different motion cues that are considered in this study are listed in Table 1, together with the associated human motion perception sensor and the relation between the effective sensor output and the pitch attitude and its derivatives. Rotational pitch motion cues are perceived with the semicircular canals. Semicircular canal dynamics are such that they yield a sensation of pitch rate $\dot{\theta}$, while they actually react to pitch acceleration [2].

Otoliths are sensitive to specific forces, which during pitch maneuvers are a result of the heave acceleration $a_z$ and tilting of the gravity vector. The tilting of the gravity vector introduces an additional longitudinal component and a reduction in the vertical component of specific force. For the relatively small pitch angles considered in this study, however, the dynamic contribution of gravity to the specific force is believed to be minor compared with that of linear body acceleration. Therefore, only the heave accelerations are considered to yield significant changes in specific force, as sensed by otoliths.

As pitch heave motion is directly related to changes in pitch [Eq. (1)] and the otolith dynamics are more or less a gain in the frequency range of interest [2], the pitch heave motion is believed to yield a sensation proportional to the pitch acceleration $\ddot{\theta}$. The center of gravity heave (CH) is related to both the pitch rate and pitch attitude, as can be verified from Table 1 and Fig. 4. The significant phase shift reduces the correlation of this motion cue with the controlled pitch attitude.

## III. Optimal Control Analysis

All motion cues during pitch maneuvers can, to some extent, be related to the pitch attitude $\theta$ and its derivatives. To investigate how pitch rate and pitch acceleration information can be used optimally to improve performance in a pitch attitude control task, an optimal control analysis is performed. An analogy can be made between a human controller and an optimal controller [17], if we consider the human controller to be well trained and operating in optimal conditions.

**Table 1 Pitch maneuvering motion cues related to pitch derivatives**

| Motion cue | Motion sensor | Sensor input | Effective sensor output |
|---|---|---|---|
| Pitch | Semicircular canals | Pitch acceleration, $\ddot{\theta}$ | Pitch rate, $\dot{\theta}$ |
| Pitch heave | Otoliths | Heave acceleration, $a_{z_\theta}$ | Pitch acceleration, $\ddot{\theta}$ |
| C.g. heave | Otoliths | Heave acceleration, $a_{z_{cg}}$ | Pitch rate, $\dot{\theta}$ (low freq., 90 deg phase shift w.r.t. $\theta$)<br>Pitch attitude, $\theta$ (higher freq., 90–180 deg phase shift w.r.t. $\theta$) |

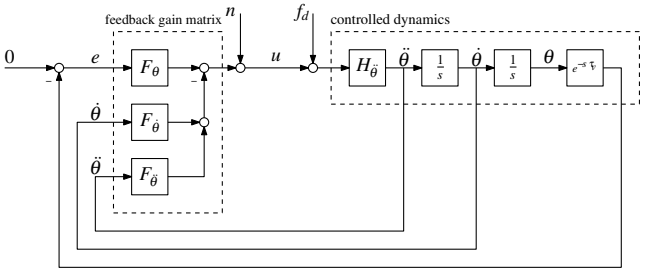


**Fig. 5 Optimal linear regulator feedback structure.**

### A. Setup of the Optimal Control Model

The closed-loop linear regulator feedback structure used in the optimal control analysis is given in Fig. 5. This feedback structure represents a pitch disturbance-rejection task, in which the pitch angle of the aircraft needs to be minimized. The aircraft dynamics are given by Eq. (2). To investigate the influence of some of the pilot limitations, a remnant signal $n$ is added to the control signal $u$ and an additional time delay $\tau_v$ is included into the pitch channel. The remnant is low-pass filtered white noise, with filter characteristics given by $K_n/(0.1s+1)^2$, where the gain $K_n$ is varied to yield different noise intensities [15]. As pitch angle is mainly perceived visually, the additional time delay is included to simulate the generally larger time delay in visual perception, compared with vestibular perception [2,18]. The optimal control law is given by

$$u = -F_\theta\theta - F_{\dot\theta}\dot\theta - F_{\ddot\theta}\ddot\theta \tag{4}$$

where the optimal values for the feedback gains $F$ are found by minimizing the following criterion:

$$J = \underbrace{Q_1\sigma^2(\theta) + Q_2\sigma^2(\dot\theta) + Q_3\sigma^2(\ddot\theta)}_{\text{performance}} + \underbrace{R\sigma^2(u)}_{\text{effort}} \tag{5}$$

In the criterion function, gains $Q$ and $R$ are weighing factors for the variance of pitch attitude and rates (tracking performance) and the variance of the control signal (control effort), respectively. In the remainder of the analysis $Q_1$, $Q_2$, and $Q_3$ are set to 1, that is, the pitch attitude and its rates are weighed equally.

### B. Results

The results of the optimal control analysis give insight into the optimal use of pitch angle, pitch rate, and pitch acceleration information in a pitch control task. As pitch heave and center of gravity heave are related to pitch acceleration and pitch rate, the optimal control analysis also provides insight into the possible use of the aircraft heave motion in this task.

First, optimizations were performed with an increasing weighing factor for the control effort, that is, forcing reduced control effort. Both the remnant signal and the additional time delay were set to 0. From Fig. 6, it can be seen that by increasing the weight on control effort the variance of the control signal decreases. As a consequence, the variance of the pitch angle, pitch rate, and pitch acceleration are seen to increase, indicative of reduced tracking performance. If the

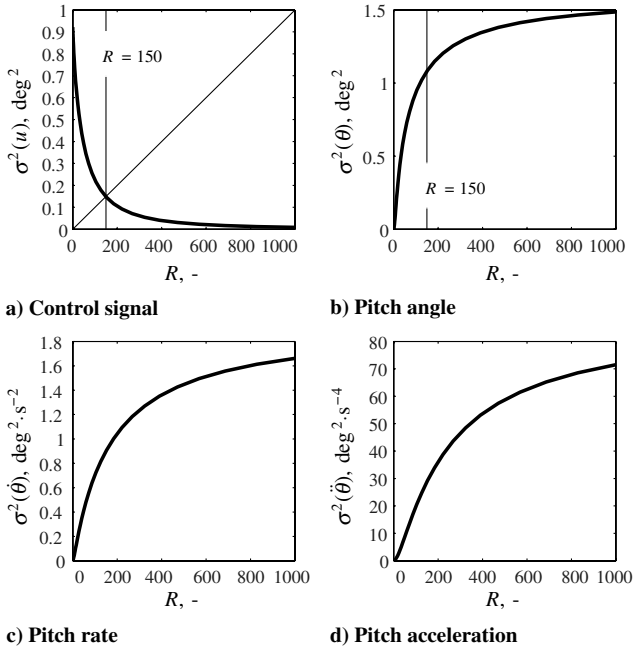


**Fig. 6 Variance of the signals for an increase in the control signal weighing factor.**

control effort increases ($R$ approaches 0), the control performance will also increase. In Fig. 7a, the optimal control gains for an increase in the control effort weighing factor are given. For the highest performance ($R < 150$), pitch acceleration feedback is the most important (highest feedback gain) and pitch rate feedback is the least important. For reduced control activity ($R > 150$), pitch rate becomes the most important and pitch angle feedback the least important.

Figure 7b shows that, when a tradeoff between performance and control effort is considered ($R \approx 150$), an increase in the pitch attitude time delay results in an increase in the pitch rate feedback gain. The feedback gains for the pitch attitude and pitch acceleration remain nearly constant. Figure 7c shows that an increase in pilot remnant intensity will increase all the feedback gains, but the gain for the pitch rate feedback increases more rapidly.

### C. Discussion

As explained in Sec. II, in a pitch control task, the total aircraft motion can be decomposed into pitch motion, pitch heave, and center of gravity heave components. This analysis shows that pitch motion, providing information on pitch rate due to the integrating characteristics of the semicircular canals, will be the most important motion component available to the pilot ($R \approx 150$). Also, increasing the remnant power or the pitch angle time delay warrants an increasing need for pitch motion. Pitch heave motion, providing information on pitch acceleration, is also an important feedback component. With increasing levels of remnant, the use of this motion

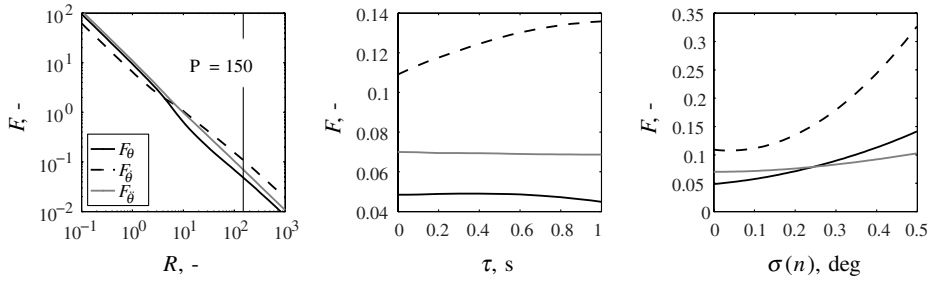


**Fig. 7 Optimal feedback gains.**

component becomes less important compared with the other motion components.

The center of gravity heave motion also provides pitch rate information at lower frequencies, but with an additional phase shift. Because of this, the usefulness of center of gravity heave in a pitch control task is less evident. The control task described in this paper typically contains high-frequency content. This suggests that center of gravity heave is likely to be the least useful motion component.

## IV. Experiment

To investigate the effects of pitch and heave motion on pilot control behavior and performance in an aircraft pitch control task, a human-in-the-loop experiment was performed in the SIMONA Research Simulator (SRS) at Delft University of Technology. This experiment was designed to yield conclusions on the relative importance of these different types of motion cues that are available during aircraft pitch maneuvers.

### A. Method

#### 1. Forcing Functions

The experiment required participants to perform a closed-loop pitch attitude control task as defined in Sec. II and Fig. 2. The target and disturbance signals that were inserted into the closed-loop system were designed as quasi-random sums of sines with independent sine frequencies for identification purposes. For instance, the target forcing function $f_t$ was generated according to

$$f_t(t) = \sum_{k=1}^{N_t} A_t(k) \sin(\omega_t(k)t + \phi_t(k)) \tag{6}$$

In Eq. (6), $A_t(k)$, $\omega_t(k)$, and $\phi_t(k)$ indicate the amplitude, frequency, and phase of the $k$th sine in $f_t$; and $N_t$ indicates the number of sines in the target signal. The disturbance signal was defined by a similar equation, only with different amplitude, frequency, and phase distributions. Both $f_d$ and $f_t$ consisted of 10 individual sinusoids.

The measurement time of an individual measurement run during the experiment was $T_m = 81.92$ s. The sinusoid frequencies $\omega_d(k)$ and $\omega_t(k)$ were all defined to be integer multiples of the measurement time base frequency, $\omega_m = 2\pi/T_m = 0.0767$ rad/s. The selected sinusoid frequencies and the corresponding integer factors of $\omega_m$, indicated by the symbols $n_d$ and $n_t$, can be found in the first two columns for $f_d$ and for $f_t$ in Table 2.

For the amplitudes of the individual sines, a second-order low-pass distribution was selected. Such a low-pass signal characteristic ensures reduced power at the higher frequencies, yielding a realistic and not overly difficult tracking task. The absolute value of the filter defined in Eq. (7) at a sinusoid frequency gives the corresponding sinusoid amplitude:

$$H_A(j\omega) = \frac{(1 + T_{A_1} j\omega)^2}{(1 + T_{A_2} j\omega)^2} \tag{7}$$

where $T_{A_1} = 0.1$ s and $T_{A_2} = 8.0$ s.

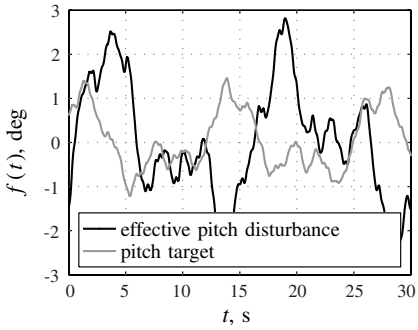


**Fig. 8 Sample time trace of the effective disturbance and target forcing function signals.**

The filter defined by Eq. (7) was used for generating the amplitudes of both $f_d$ and $f_t$. The amplitude distributions $A_d(k)$ and $A_t(k)$ were then scaled to attain variances for $f_d$ and $f_t$ of 1.6 and 0.4 deg$^2$, respectively. The reduced magnitude of the target signal ensured that the closed-loop tracking task performed in the experiment was primarily a disturbance-rejection task. Figure 8 depicts a part of the time traces of both these signals.

To determine the forcing function phase distributions, a large number of random sets of phases was generated. The two sets of phases that yielded signals with a probability distribution closest to a Gaussian distribution, without leading to excessive peaks, were selected for $f_d$ and $f_t$ [13].

The disturbance forcing function was designed as a realistic disturbance on the aircraft pitch attitude $\theta$. However, as can be verified from Fig. 2, the disturbance signal was inserted into the closed-loop control task *before* the controlled aircraft dynamics by adding it to the subject's control signal $u$. Therefore, the disturbance signal amplitudes and phases were preshaped with the inverse of the aircraft model pitch response $H_{\theta,\delta_e}(j\omega)$. This ensured that $f_d$ caused an effective pitch attitude disturbance as depicted in Fig. 8. The properties of the target and disturbance signals are summarized in Table 2.

#### 2. Independent Variables

The experiment was designed to investigate the effect of three different types of motion cues on pilot pitch attitude control behavior. Therefore, the independent variables in the experiment were the three types of motion cues that were thought to be important during pitch maneuvers (see also Fig. 1): 1) rotational pitch motion, 2) vertical pitch heave motion, and 3) vertical c.g. heave motion.

The experiment had a full factorial design in which all three types of motion could be either on or off. This gave a total of eight experimental conditions, which are listed in Table 3. Note that conditions C1–C4 are the conditions without pitch motion for which the available heave cues vary from 1) no heave to 2) pitch heave, 3) c.g. heave, and 4) both types of heave. Conditions C5–C8 are the corresponding heave conditions with additional rotational pitch motion.

**Table 2 Experiment forcing function properties**

| Disturbance, $f_d$ | | | | Target, $f_t$ | | | |
|---|---|---|---|---|---|---|---|
| $n_d$ | $\omega_d$, rad · s$^{-1}$ | $A_d$, deg | $\phi_d$, rad | $n_t$ | $\omega_t$, rad · s$^{-1}$ | $A_t$, deg | $\phi_t$, rad |
| 5 | 0.383 | 0.344 | −1.731 | 6 | 0.460 | 0.698 | 1.288 |
| 11 | 0.844 | 0.452 | 4.016 | 13 | 0.997 | 0.488 | 6.089 |
| 23 | 1.764 | 0.275 | −1.194 | 27 | 2.071 | 0.220 | 5.507 |
| 37 | 2.838 | 0.180 | 4.938 | 41 | 3.145 | 0.119 | 1.734 |
| 51 | 3.912 | 0.190 | 5.442 | 53 | 4.065 | 0.080 | 2.019 |
| 71 | 5.446 | 0.235 | 2.274 | 73 | 5.599 | 0.049 | 0.441 |
| 101 | 7.747 | 0.315 | 1.636 | 103 | 7.900 | 0.031 | 5.175 |
| 137 | 10.508 | 0.432 | 2.973 | 139 | 10.661 | 0.023 | 3.415 |
| 171 | 13.116 | 0.568 | 3.429 | 194 | 14.880 | 0.018 | 1.066 |
| 226 | 17.334 | 0.848 | 3.486 | 229 | 17.564 | 0.016 | 3.479 |

**Table 3 Experimental conditions**

| Condition | Simulator motion | | |
|---|---|---|---|
| | Pitch | Pitch heave | C.g. heave |
| C1 | − | − | − |
| C2 | − | + | − |
| C3 | − | − | + |
| C4 | − | + | + |
| C5 | + | − | − |
| C6 | + | + | − |
| C7 | + | − | + |
| C8 | + | + | + |

*3. Apparatus*

The experiment was conducted in the SRS at Delft University of Technology (see Fig. 9). This simulator has a 6 degree-of-freedom hydraulic hexapod motion system capable of a maximum pitch rotation of ±24 deg and a maximum vertical stroke of around 130 cm. The time delay of the motion system is 30 ms [19].

During the experiment, subjects were seated in the right pilot seat. An active electrical sidestick without breakout force was used to give elevator control inputs to the Citation aircraft model defined by Eq. (2) and (3). Only pitch commands could be given as the stick roll axis was fixed. A scale factor controlled the gain of the sidestick such that 1 deg of stick pitch deflection resulted in an elevator deflection, $\delta_e$, of $-0.2865$ deg.

For presenting the tracking error $e$, a simplified artificial horizon image was depicted on the primary flight display (PFD) directly in front of the subjects. As shown in Fig. 10, the vertical distance between the horizon line and the aircraft symbol depicted on this artificial horizon image indicated the magnitude of the tracking error. The update rate of the PFD was 60 Hz. From previous experiments it is known that the latency of SIMONA's primary flight displays, including the projection, is no more than 25 ms [4].

Physical motion was generated using the pitch and heave degrees of freedom of the SRS motion base. As the forcing functions were designed such that the aircraft model pitch attitude during the experiment would rarely exceed 5 deg, it was decided to use no motion filter for generating the rotational pitch motion. For the heave motion cues, a motion filter was required, as especially the low-pass c.g. heave motion would otherwise yield heave excursions that would far exceed the SRS limits. To attenuate especially the very low-frequency large-amplitude portion of the heave motion, a third-order high-pass filter similar to those used in classical washout filters was implemented [20]:

$$H_{mf}(s) = K_{mf}\left(\frac{s^2}{s^2 + 2\zeta_{n_{mf}}\omega_{n_{mf}}s + \omega_{n_{mf}}^2}\right)\left(\frac{s}{s + \omega_{b_{mf}}}\right) \quad (8)$$

The selected parameters for this third-order filter were tuned to ensure that the c.g. heave motion remained within the motion-base limits, whereas the much-lower amplitude pitch heave motion would still be clearly perceivable. This resulted in the motion filter parameter set listed in Table 4. Note that, compared with a previous experiment [21], both the filter gain and the second-order breakout frequency were increased from 0.3 to 0.6 and from 0.4 to 1.25 rad/s, respectively. These motion filter parameters were found to yield a much better balance between the pitch heave and c.g. heave accelerations and an overall realistic aircraft pitch maneuvering motion profile.

To mask the acoustic noise made by the motion-base actuators, participants wore a noise-canceling headset. Even with this headset on, the noise produced by the sliding actuators during conditions with c.g. heave, that is, during large-amplitude heave motion, was still found to be audible. Therefore, an additional masking sound (aircraft engine noise) was played over the headphones to conceal any remaining motion-base sounds.


**Fig. 9 The SIMONA Research Simulator.**

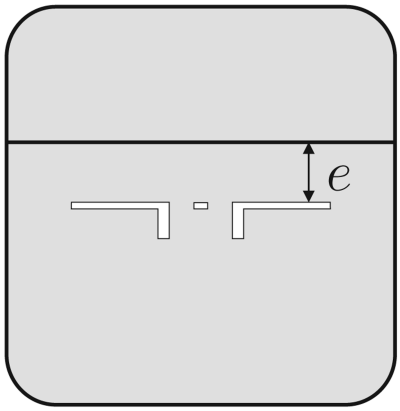


**Fig. 10 Compensatory display.**

*4. Subjects and Instructions*

Seven subjects were invited to perform this experiment, all students or staff of the Faculty of Aerospace Engineering. All had experience with similar manual control tasks from previous human-in-the-loop experiments. Two subjects have additional experience as aircraft pilots; one of them is an experienced single- and multi-engine aircraft pilot. The subjects' ages ranged from 25 to 46 years old.

Before starting the experiment, the subjects received an extensive briefing on the scope and objective of the experiment. They were informed that they would be subjected to the different motion configurations listed in Table 3. The main instruction they received before the experiment was to attempt to minimize the pitch tracking error, that is, the signal that was presented on the visual display, as best as possible.

*5. Experimental Procedure*

Immediately after the participants received their instructions, the experiment started with a considerable number of training runs. During the entire experiment, that is, both during the training and measurement runs, the eight conditions of the experiment were presented in random order according to a balanced Latin square design. Typically, each subject performed two repetitions of all conditions (16 runs) in between breaks.

No separate subdivision between the training and measurement runs was made beforehand. Tracking performance was tracked by the experimenter during the entire experiment. When the subjects' levels of performance had clearly stabilized and five repetitions of each condition had been collected at this stable performance level,

**Table 4 Heave motion filter parameters**

| Parameter | Value | Unit |
|---|---|---|
| $K_{mf}$ | 0.6 | —— |
| $\omega_{n_{mf}}$ | 1.25 | rad · s$^{-1}$ |
| $\zeta_{n_{mf}}$ | 0.7 | —— |
| $\omega_{b_{mf}}$ | 0.3 | rad · s$^{-1}$ |

the experiment was terminated. On average, 8–9 repetitions of each experimental condition were sufficient for each subject to gather the measurement data.

Each experiment run lasted 110 s, of which the final 81.92 s were used as the measurement data. Participants generally needed some time to stabilize the disturbed aircraft model after the start of a run; therefore, the data from the first 28.08 s of each run were discarded. Data were logged at a frequency of 100 Hz.

After each run, subjects were informed of their tracking score, expressed in terms of the rms of the error signal $e$, to motivate them to constantly control at their maximum level of performance.

For a comparison with the results of an earlier experiment [21], subjects were asked to indicate if they had perceived pitch and heave motion after each run. These subjective reporting data were recorded by the experimenter before the next run was started.

#### 6. *Dependent Measures*

The dependent measures consisted, first of all, of the subjective pitch and heave reporting data. In addition, the pitch attitude $\theta$ and its derivatives, the vertical acceleration $a_z$, the tracking error signal $e$, and the control signal $u$, were recorded during each run. From these objective measurements, a number of other dependent measures were calculated.

First of all, the variances of the error ($e$) and control signals ($u$) were considered as measures of pilot tracking accuracy and control activity, respectively. In addition, the recorded experiment time histories were used to obtain pilot describing functions and to estimate the parameters of a structural pilot model from the measurement data. The pilot model used for this experiment will be introduced in Sec. V. Pilot–model parameters are used to objectively evaluate changes in pilot control strategy. In addition, pilot–aircraft system crossover frequencies and phase margins are evaluated as frequency domain measures of pilot performance and stability.

### B. Hypotheses

Based on the optimal control analysis described in Sec. III, the following hypotheses on the use of pitch rotation, pitch heave, and center of gravity heave in a pitch control task were derived.

First, it is hypothesized that pitch motion will be the most important cue to achieve high performance in a pitch control task. This was also found in previous research [11,22] and is supported by the optimal control analysis discussed in Sec. III, which showed the highest feedback gain for the pitch rate, that is, the output from the semicircular canals.

Second, pitch heave is also hypothesized to be an important cue for high performance. Despite the fact that most previous research suggests that heave motion has a minor effect on performance [8,11], the optimal control analysis provides a larger feedback gain for pitch acceleration compared with pitch angle feedback.

Center of gravity heave has a less straightforward relationship with the controlled pitch attitude. Therefore, as a final hypothesis, center of gravity heave is thought to be the least important motion cue in a pitch control task.

**Table 5 ANOVA results of performance and control activity, where ** is highly significant ($p < 0.01$), * is significant ($0.01 \leq p < 0.05$), and - is not significant ($p \geq 0.05$).**

| Independent variables | | Dependent measures | | | | | |
|---|---|---|---|---|---|---|---|
| | | $\sigma^2(e)$ | | $\sigma^2(u)$ | | $\sigma^2(\theta)$ | |
| Factor | df | F | Sig. | F | Sig. | F | Sig. |
| P | 1, 6 | 466.9 | ** | 2.4 | - | 72.3 | ** |
| PH | 1, 6 | 15.1 | ** | 1.9 | - | 17.4 | ** |
| CH | 1, 6 | 1.2 | - | 4.1 | - | 4.8 | - |
| P × PH | 1, 6 | 9.1 | * | 0.1 | - | 0.6 | - |
| P × CH | 1, 6 | 4.6 | - | 6.9 | * | 8.4 | * |
| PH × CH | 1, 6 | 3.8 | - | 3.3 | - | 0.7 | - |
| P × PH × CH | 1, 6 | 2.6 | - | 0.0 | - | 3.2 | - |

## V. Results

This section presents the combined results of the seven subjects who participated in the experiment. First, the motion reporting results will be described. Second, tracking performance and control activity will be analyzed using the time-domain data from all the experiment runs. Next, pilot control behavior will be identified in the frequency domain using a multimodal pilot model. The results are analyzed using a repeated-measures analysis of variance (ANOVA) to reveal any significant effects.

### A. Motion Reporting

After each run, the subjects were asked to report if they experienced any pitch or heave motion. No distinction had to be made between pitch heave or center of gravity heave. With a few exceptions, almost all of the pitch and heave reports were correct for every condition and every subject. This is in contrary to the results found in a previous experiment [21], in which a significant number of reports was incorrect for a highly similar task. This is thought to be due to the different trim condition of the aircraft model, which forced the motion filters of the simulator to be tuned down considerably. The reporting results found in the current experiment suggest that the motion was tuned more optimally and that all motion cues were clearly distinguishable.

### B. Tracking Performance and Control Activity

Figure 11 gives the variances of the error, control, and pitch signal for all conditions averaged over seven subjects. The variances are partitioned into variance components due to the target forcing function, the disturbance forcing function, and the remnant [23]. The corresponding ANOVA results for the variances are given in Table 5.

The variance of the error signal, given in Fig. 11a, is a measure of pilot control performance. For the error signal, the variance due to the target forcing function is much smaller than the variance due to the disturbance. This can be explained by the fact that the target forcing function is scaled to a quarter of the power of the disturbance forcing function at the error signal (see Sec. IV).

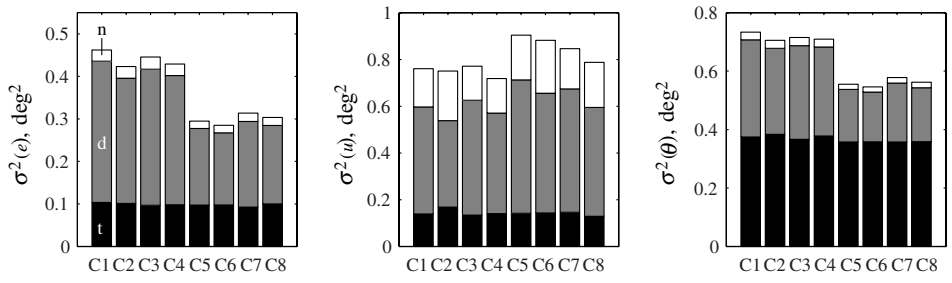


**a) Error signal** **b) Control signal** **c) Pitch signal**

**Fig. 11 Variance decomposition of the experiment variables for every condition averaged over seven subjects. The black bars are the variance due to the target forcing function ($t$), the gray bars the variance due to the disturbance forcing function ($d$), and the white bars the variance due to the pilot remnant ($n$).**

It can be seen that, for conditions with pitch motion, the subjects were able to attain a much higher level of performance than for conditions without pitch motion. This effect was highly significant, as can be judged from Table 5. As can be clearly seen in Fig. 11a, the reduction in variance of the error signal is mainly due to the significant reduction of the variance caused by the disturbance forcing function ($F(1,6) = 477.5,\ p < 0.01$). The target forcing function component was not significantly affected ($F(1,6) = 1.0,\ p \geq 0.05$). The addition of pitch heave also had a highly significant effect on performance (see Table 5). The subjects achieved a higher performance with pitch heave motion, again by a reduction of the disturbance variance in the error signal ($F(1,6) = 18.2,\ p < 0.01$). There was no significant effect for the target variance component ($F(1,6) = 1.3,\ p \geq 0.05$). Center of gravity heave was found to have no significant effect on the pilot performance. In addition to these main effects, the ANOVA also revealed a significant interaction between pitch motion and pitch heave motion. If no pitch motion is present, there is a bigger increase in performance due to pitch heave (C1 and C3 compared with C2 and C4) than to pitch motion (C5 and C7 compared with C6 and C8).

Figure 11b shows the variance of the pilot control signal, a measure for pilot control activity. Although from this figure a higher control activity for the conditions with pitch motion can be observed, the effect is not significant (see Table 5). The increase in variance for the pitch motion conditions is a combination of an increase of the disturbance variance and the remnant variance. There is no significant effect resulting from the different heave conditions. The only significant effect on pilot control activity is due to the interaction between pitch motion and center of gravity heave. This implies that the increase in control activity due to pitch motion is smaller if center of gravity heave is present.

A decomposition of the variance for the pitch angle is given in Fig. 11c. For the pitch angle, the variance due to the target forcing function is much bigger than the variance due to the disturbance, especially compared with the error signal $e$. This is caused by the fact that the target is actively tracked by the pilot and the disturbance is minimized. The addition of pitch motion and pitch heave motion results in a highly significant reduction in the variance of the pitch angle. As for the error signal, this is due to a reduction of the variance caused by the disturbance component ($F(1,6) = 477.5,\ p < 0.01$ for pitch motion and $F(1,6) = 18.2,\ p < 0.01$ for pitch heave). There was no significant effect for the target variance component caused by pitch motion ($F(1,6) = 1.7,\ p \geq 0.05$) or by pitch heave ($F(1,6) = 2.5,\ p \geq 0.05$). There is a significant interaction between pitch motion and center of gravity heave. If there is no center of gravity heave, the addition of pitch motion causes a larger reduction in pitch variance than found in conditions with center of gravity heave.

### C. Pilot Control Behavior

#### 1. *Identification Procedure*

For some conditions of the current experiment, both pitch and heave motion cues were presented in addition to the visual cues. This warrants the use of a three-channel pilot model separating the response into visual, pitch motion, and heave motion cues. In such a model, the pitch motion channel consists of the semicircular canal dynamics and the heave motion channel of the otolith dynamics. Such a three-channel model was found to provide inaccurate estimation results, as the pilot response to heave cues was marginal in magnitude compared with the other motion cues. This could also be expected by observing the relatively small effects of heave motion in the variance analysis given in the previous section. Instead, a model with only two channels was used, and the response to heave cues was left unmodeled. The structure of this model is given in Fig. 12. For conditions without pitch motion only the pilot visual response $H_{pe}$ was modeled.

Human operators adapt their control behavior to the controlled dynamics, $H_{\theta,\delta_e}$, in such a way that the open-loop dynamics in the crossover region can be described by a single integrator and a time delay [24]. The aircraft dynamics in Fig. 3 suggest that the pilot needs

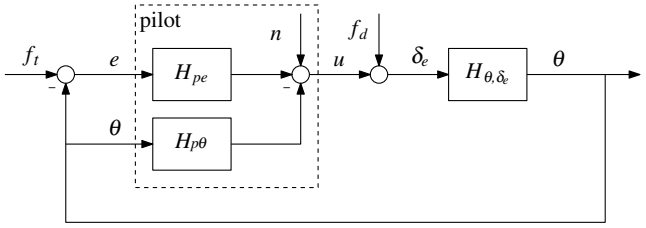


**Fig. 12 Multiloop structure used for identification of control behavior.**

to generate lag to compensate for the gain dynamics below the short period frequency. In addition, a high-frequency lead is needed to compensate for the double-integrator dynamics above the short period frequency. To model this transition in pilot equalization around the short period frequency, a double-lead term was found to be required. The best estimation results were obtained for a pilot model in which both lead time constants had the same value. Based on McRuer and Jex's precision model [24] and van der Vaart's multichannel model [3], the linear response functions $H_{pe}$ and $H_{p\theta}$ (see Fig. 12) are then parameterized by

$$H_{pe}(j\omega) = K_v \frac{(1 + j\omega T_{\text{lead}})^2}{(1 + j\omega T_{\text{lag}})} e^{-j\omega\tau_v} H_{nm}(j\omega) \tag{9}$$

$$H_{p\theta}(j\omega) = (j\omega)^2 H_{sc}(j\omega) K_m e^{-j\omega\tau_m} H_{nm}(j\omega) \tag{10}$$

In the visual perception channel, $H_{pe}$, $K_v$ is the visual perception gain, $T_{\text{lead}}$ the visual lead time constant, $T_{\text{lag}}$ the visual lag time constant, and $\tau_v$ the visual perception time delay. The pitch motion perception channel, $H_{p\theta}$, includes the dynamics of the semicircular canals $H_{sc}$, the motion perception gain $K_m$, and a motion perception time delay $\tau_m$. The control action of the pilot is limited by the neuromuscular dynamics $H_{nm}$, given by

$$H_{nm}(j\omega) = \frac{\omega_{nm}^2}{\omega_{nm}^2 + 2\zeta_{nm}\omega_{nm} j\omega + (j\omega)^2} \tag{11}$$

with $\zeta_{nm}$ the neuromuscular damping and $\omega_{nm}$ the neuromuscular frequency. The semicircular canal dynamics in the pitch motion perception channel are given by

$$H_{sc}(j\omega) = \frac{1 + j\omega T_{sc1}}{1 + j\omega T_{sc2}} \tag{12}$$

where $T_{sc1} = 0.1$ s and $T_{sc2} = 6.0$ s are the lead and lag time constants of the semicircular canals, respectively. These values are taken from previous research [2] and are kept fixed in the parameter estimation procedure. This leaves a total of eight parameters to be estimated ($K_v, T_{\text{lead}}, T_{\text{lag}}, \tau_v, K_m, \tau_m, \zeta_{nm}, \omega_{nm}$).

The pilot model was fit in the frequency domain using an autoregressive exogenous (ARX) model estimate of the disturbance open-loop and the target open-loop [15,23]. Using the response functions given in Fig. 12, the disturbance open-loop is given by

$$H_{ol,d}(j\omega) = \frac{U(j\omega)}{\delta_e(j\omega)} = [H_{pe}(j\omega) + H_{p\theta}(j\omega)] H_{\theta,\delta_e}(j\omega) \tag{13}$$

and the target open-loop is given by

$$H_{ol,t}(j\omega) = \frac{\theta(j\omega)}{E(j\omega)} = \frac{H_{pe}(j\omega) H_{\theta,\delta_e}(j\omega)}{1 + H_{p\theta}(j\omega) H_{\theta,\delta_e}(j\omega)} \tag{14}$$

The ARX estimates were calculated using the averaged time traces from five runs of the error, the pitch angle, and the control signal. An example of the estimated open-loop frequency response functions from the ARX model and the pilot parameter model are given in Fig. 13. This figure also gives the Fourier coefficients (FC) for the two open-loop cases. It can be seen that the fit of the parameter model is very accurate for the whole frequency range.

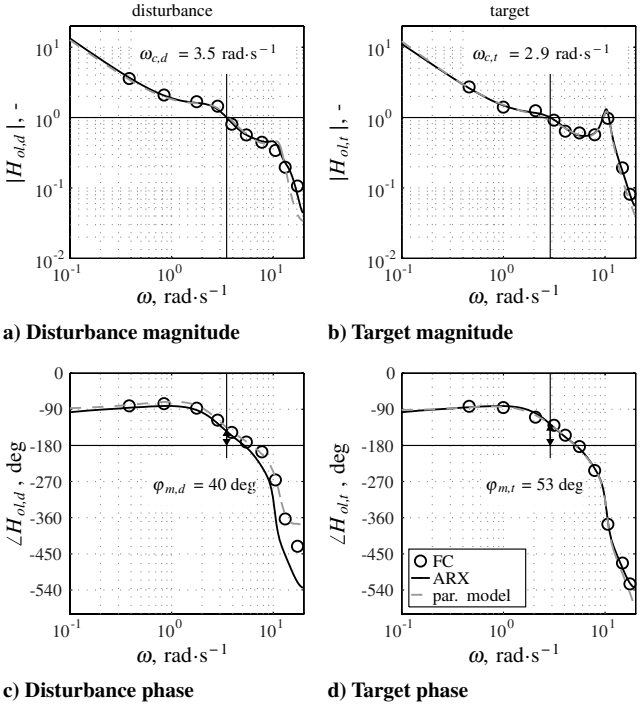


**a) Disturbance magnitude** **b) Target magnitude**

**c) Disturbance phase** **d) Target phase**

**Fig. 13 Open-loop frequency response functions (subject 1, condition 5).**

The resulting frequency response functions of the pilot model are given in Fig. 14. This figure also shows a good resemblance between the ARX model and the parameter model, except for a small misfit for the pitch motion response function.

### 2. *Crossover Frequencies and Phase Margins*

A control task with both a target and a disturbance forcing function yields a closed-loop system whose performance depends on attenuating the errors introduced by both these forcing function signals. This implies that two open-loop responses and also two crossover frequencies and phase margins need to be considered for such a task [23]. Figure 15 gives the error-bar plots of the crossover

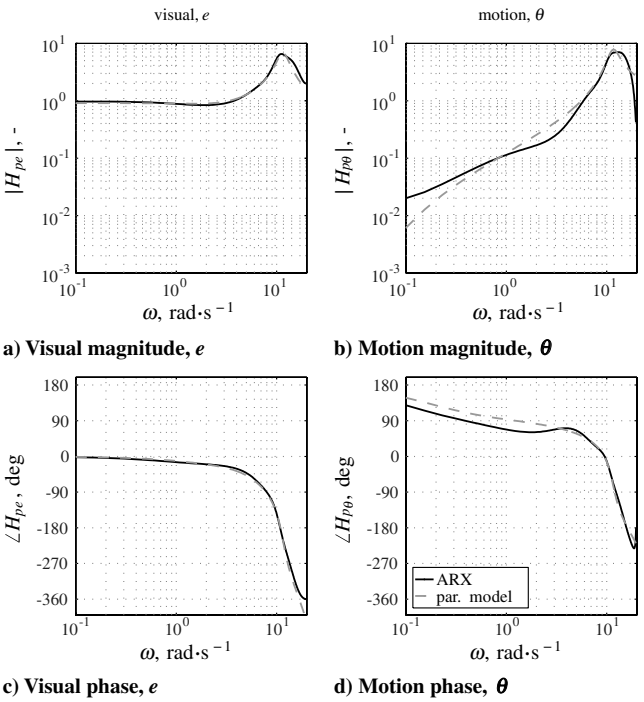


**a) Visual magnitude, $e$** **b) Motion magnitude, $\theta$**

**c) Visual phase, $e$** **d) Motion phase, $\theta$**

**Fig. 14 Pilot frequency response functions (subject 1, condition 5).**

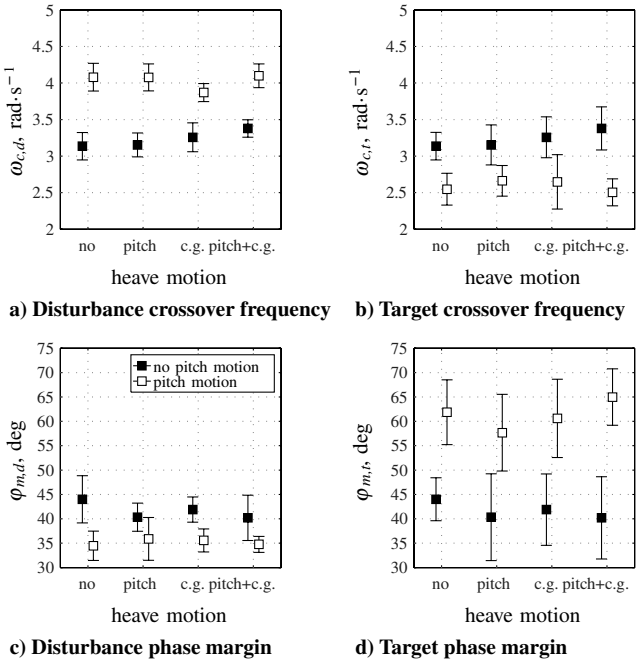


**a) Disturbance crossover frequency** **b) Target crossover frequency**

**c) Disturbance phase margin** **d) Target phase margin**

**Fig. 15 Crossover frequencies and phase margins.**

frequencies and phase margins for the target and disturbance open loop for all conditions. The error bars give the 95% confidence intervals of the means over seven subjects. Note that the error bars have been corrected by adjusting the subject means to account for between-subject effects.

Table 6 provides the ANOVA results for the crossover frequencies and phase margins. From this table it can be observed that pitch motion is the only main effect producing significant results. For the target open loop the runs with pitch motion have a significantly lower crossover frequency, whereas the phase margin significantly increases. This shows that, for target following, pitch motion causes a small reduction in performance and a much higher stability. For the disturbance open loop the crossover frequency significantly increases and the phase margin slightly decreases with pitch motion. This implies better disturbance suppression for the conditions with pitch motion, while slightly decreasing stability. These effects on crossover frequency and phase margin for target and disturbance loops, with and without motion, are found in many previous experiments [2–4,23].

The interaction between pitch motion and center of gravity heave also has a significant effect on the crossover frequencies and the phase margin for the target open loop (see Table 6). For the target loop the decrease in crossover frequency and the increase in phase margin with pitch motion is larger when center of gravity heave is present. In contrast, for the disturbance loop the increase in crossover frequency is larger without center of gravity heave.

### 3. *Pilot–Model Parameters*

Figure 16 gives the error-bar plots of the estimated pilot–model parameters for all conditions. The error bars indicate the 95% confidence intervals of the means over seven subjects. The plots are corrected for between-subject effects. The ANOVA results for the pilot–model parameters are given in Table 7.

From Fig. 16, an increase in visual perception gain $K_v$ can be observed when pitch motion is added, indicating that subjects responded more strongly to visual cues. A higher visual gain reduces both target and disturbance errors. This effect is also found in previous experiments investigating the effects of motion on pilot control behavior [8,18], but is not significant in this experiment.

Pitch rotation, pitch heave, and center of gravity heave all had a significant effect on the value of the visual lead time constant. The visual lead constant $T_{\text{lead}}$ decreased significantly when pitch rotation and pitch heave were introduced, indicating a reduction of visual

**Table 6 ANOVA results of the crossover frequencies and phase margins, where ** is highly significant ($p < 0.01$), * is significant ($0.01 \leq p < 0.05$), and - is not significant ($p \geq 0.05$).**

| Independent variables | | Dependent measures | | | | | | | |
|---|---|---|---|---|---|---|---|---|---|
| | | $\omega_{c,d}$ | | $\omega_{c,t}$ | | $\varphi_{m,d}$ | | $\varphi_{m,t}$ | |
| Factor | df | F | Sig. | F | Sig. | F | Sig. | F | Sig. |
| P | 1, 6 | 74.8 | ** | 11.5 | * | 23.6 | ** | 12.9 | * |
| PH | 1, 6 | 4.0 | - | 0.4 | - | 0.9 | - | 1.2 | - |
| CH | 1, 6 | 0.6 | - | 2.7 | - | 0.4 | - | 0.6 | - |
| P × PH | 1, 6 | 1.1 | - | 3.0 | - | 5.0 | - | 3.2 | - |
| P × CH | 1, 6 | 17.8 | ** | 9.5 | * | 0.4 | - | 8.7 | * |
| PH × CH | 1, 6 | 4.1 | - | 1.2 | - | 0.0 | - | 5.9 | - |
| P × PH × CH | 1, 6 | 0.4 | - | 2.7 | - | 1.4 | - | 1.7 | - |

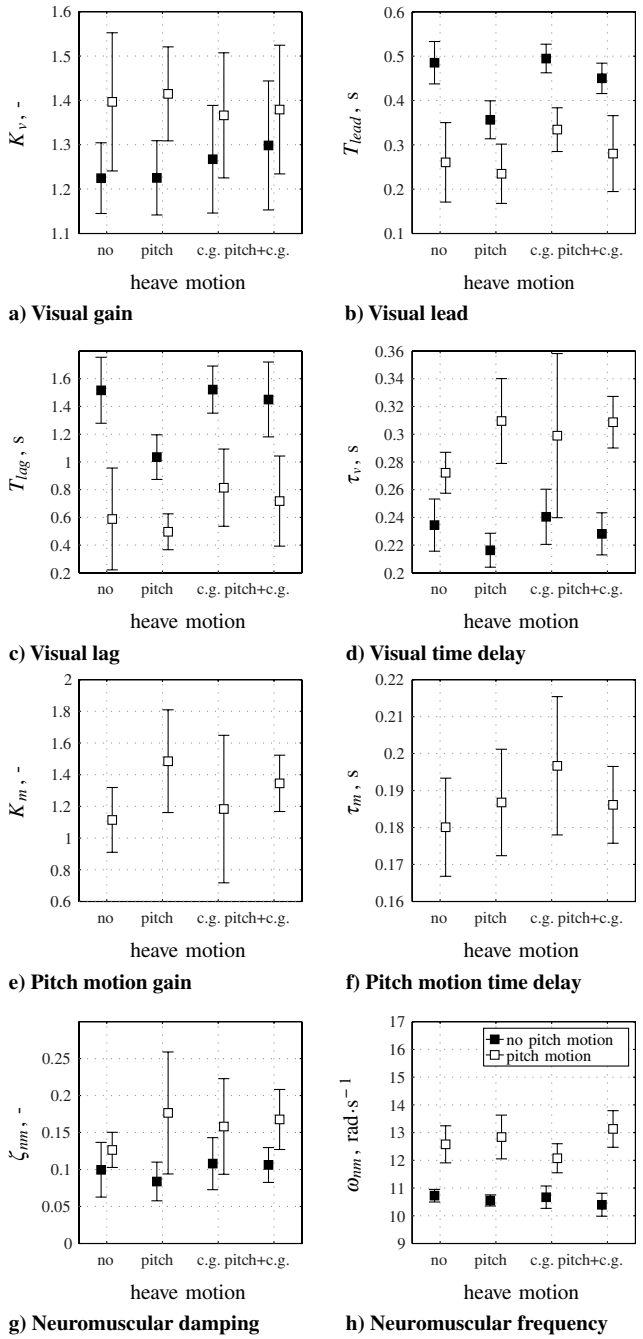


**a) Visual gain** **b) Visual lead**

**c) Visual lag** **d) Visual time delay**

**e) Pitch motion gain** **f) Pitch motion time delay**

**g) Neuromuscular damping** **h) Neuromuscular frequency**

**Fig. 16 Multimodal pilot–model parameters.**

lead, but increased when center of gravity heave was introduced. Typically, motion cues reduce the need for visual lead, as they provide a faster way of retrieving lead information (pitch rate) [18]. The increasing need for visual lead when center of gravity heave is added is indicative of the fact that this motion cue is not helpful during pitch control. The visual lag time constant $T_{\text{lag}}$ is also significantly affected by all three motion components. Pitch rotation and pitch heave decrease visual lag; center of gravity heave increases visual lag.

The visual time delay is only significantly affected by pitch rotation, as can be seen in Fig. 16. With pitch rotation, the need for fast processing of visual cues is less, increasing the visual time delay $\tau_v$.

The pitch motion perception gain $K_m$ and time delay $\tau_m$ are not significantly affected by the two heave components. There are also no significant effects for neuromuscular damping $\zeta_{nm}$, but a small increase in damping can be observed for the addition of pitch motion by looking at Fig. 16.

There was a highly significant effect of pitch motion on the neuromuscular frequency $\omega_{nm}$ and a significant effect of pitch heave. For both motion components the neuromuscular frequency increased. The significant effect produced by the interaction between pitch rotation and pitch heave shows an increase in neuromuscular frequency due to pitch heave for conditions with pitch rotation, but a decrease for conditions without pitch rotation (see Fig. 16h). The increase in neuromuscular frequency indicates an increase in bandwidth of the neuromuscular actuation response, resulting in higher bandwidth control. This change in neuromuscular actuation can possibly be explained by an increase in arm and hand muscle tension during the runs with pitch rotation and pitch heave.

An example of how these changes in pilot control behavior are reflected in the resulting open-loop responses is given in Fig. 17. From this figure the higher loop gain and the decrease in time delay for the disturbance open loop can be clearly seen. This allows the pilot to significantly reduce the disturbance variance component in the error and the pitch signal (see Fig. 11). As also found from other experiments that considered a task with two forcing functions [23], a second effect of the increase in loop gain due to motion cues is an increase in the magnitude of the resonance peak in the target open loop.

## VI. Discussion

Seven subjects participated in an experiment investigating the pilot's use of different types of motion cues in a pitch attitude control task, with simultaneous target and disturbance inputs.

Pitch rotational motion is found to be the most important motion cue for increasing pitch tracking performance. Adding pitch rotation caused a decrease in the disturbance variance component in the error and pitch signals, showing that subjects were better able to attenuate the disturbance. This was also seen from the crossover frequencies and phase margins. The crossover frequency of the target open loop was found to decrease slightly, whereas the disturbance open-loop crossover frequency increased strongly. Corresponding target and disturbance loop phase margins were seen to increase and decrease, respectively. With pitch motion, the visual perception gain

**Table 7 ANOVA results of the pilot–model parameters, where ** is highly significant ($p < 0.01$), * is significant ($0.01 \leq p < 0.05$), and - is not significant ($p \geq 0.05$).**

| Independent variables | | Dependent measures | | | | | | | | | | | | | | | |
|---|---|---|---|---|---|---|---|---|---|---|---|---|---|---|---|---|---|
| | | $K_v$ | | $T_{\text{lead}}$ | | $T_{\text{lag}}$ | | $\tau_v$ | | $K_m$ | | $\tau_m$ | | $\zeta_{nm}$ | | $\omega_{nm}$ | |
| Factor | df | F | Sig. | F | Sig. | F | Sig. | F | Sig. | F | Sig. | F | Sig. | F | Sig. | F | Sig. |
| P | 1, 6 | 3.0 | - | 44.4 | ** | 23.3 | ** | 31.8 | ** | | | | | 5.9 | - | 76.2 | ** |
| PH | 1, 6 | 0.2 | - | 8.3 | * | 6.9 | * | 0.2 | - | 2.0 | - | 0.1 | - | 0.4 | - | 6.9 | * |
| CH | 1, 6 | 0.1 | - | 18.6 | ** | 16.6 | ** | 1.9 | - | 0.0 | - | 0.8 | - | 0.6 | - | 0.2 | - |
| P × PH | 1, 6 | 0.0 | - | 0.8 | - | 1.1 | - | 3.3 | - | | | | | 1.6 | - | 19.8 | ** |
| P × CH | 1, 6 | 5.2 | - | 0.1 | - | 0.0 | - | 0.1 | - | | | | | 0.0 | - | 0.0 | - |
| PH × CH | 1, 6 | 0.1 | - | 0.6 | - | 2.5 | - | 0.5 | - | 0.8 | - | 1.9 | - | 1.3 | - | 0.8 | - |
| P × PH × CH | 1, 6 | 0.0 | - | 3.7 | - | 2.0 | - | 1.3 | - | | | | | 3.8 | - | 1.8 | - |

increased, although not significantly, showing a stronger reduction of both target and disturbance errors. The visual lead is reduced and the visual time delay increases, showing the pilot's preference for using the pitch motion to improve performance. Pilot neuromuscular frequency increased, indicating higher bandwidth control, possibly caused by an increased tension in the muscles of the arm controlling the sidestick.

Pitch heave motion showed the same effects on performance as pitch rotational motion, but less strongly. There were no significant trends for the crossover frequencies and phase margins, but the main effects on the pilot–model parameters, seen with the addition of pitch rotation, could also be seen for pitch heave.

Center of gravity heave motion was not used to improve performance. There were no significant trends for the variance of the signals, the crossover frequencies, and the phase margins. The pilot–model parameters even showed a significant increase in visual lead with the addition of center of gravity heave motion. This is caused by the large phase shift of the center of gravity heave at higher frequencies with respect to changes in pitch attitude, making the use of this motion cue difficult for this type of control task.

The optimal control analysis proved to give a good prediction of the importance of the different motion components. A prediction was made that pitch rate was the most important cue, followed by pitch acceleration. This is in accordance with pitch rotational motion being the most important, followed by pitch heave motion, as found in the experiment.

It should be noted that the results from this experiment depend on the type of control task, the motion filter settings, and the aircraft dynamics used. The fact that the heave motion was high-pass filtered may still have affected the influence of the pitch heave motion. In addition, the pitch heave will have a stronger positive influence on performance if the pilot station is further from the aircraft center of gravity. Typical distances from pilot station to center of gravity for large transport aircraft are on the order of 15–20 m, whereas this distance is only 3.2 m for the aircraft used in this study. With an increased pitch heave sensation at the pilot station for these larger aircraft, center of gravity heave is even less likely to be useful for improving performance because of its lower relative magnitude. Center of gravity heave could, however, still be an important factor in other aircraft control tasks, such as altitude control. These subjects are beyond the scope of this paper and will be covered in future research.

The results from this experiment suggest that, in future pitch tracking experiments, motion filter settings could be optimized by leaving out the center of gravity heave component, as it does not significantly affect tracking performance and control behavior. As center of gravity heave takes up most of the simulator motion space, leaving out this component reduces the need to filter the remaining motion components. For example, for the experiment described in this paper, no heave motion filter is, in fact, needed if center of gravity heave is left out. This strategy could also be used in motion filter tuning for tasks or phases of flight that are similar, for instance, in terms of frequency content, to the task described here.

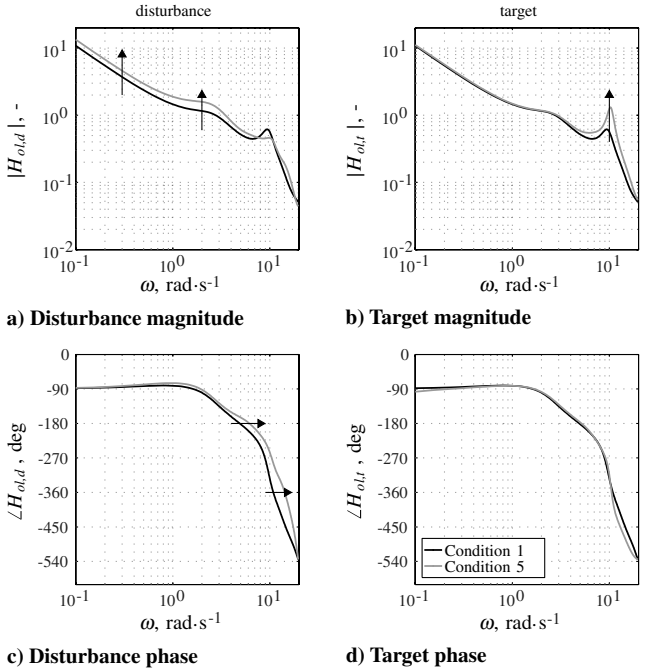


**a) Disturbance magnitude** **b) Target magnitude**

**c) Disturbance phase** **d) Target phase**

**Fig. 17 The effect of pitch motion on the open-loop frequency response functions (subject 1).**

## VII. Conclusions

In a combined pitch tracking and disturbance-rejection task, pitch motion significantly improved tracking performance, with an increased crossover frequency for the disturbance open loop. The increase in performance is a result of an increased visual gain and a reduction in visual lead, resulting in a lower effective time delay for the disturbance open loop. For the aircraft dynamics used, pitch heave motion showed effects similar to pitch rotational motion, but less strongly due, in part, to the relatively short distance of the pilot station to the center of gravity. The center of gravity heave motion cue was found to have no significant effects on performance and control behavior.

## Acknowledgments

The authors would like to thank Peter Grant and Bruce Haycock of the University of Toronto Institute for Aerospace Studies (UTIAS) for their assistance in implementing the first experiment in the UTIAS Flight Research Simulator [21]. The results of this first experiment proved to be of great value in optimizing the second experiment in the SIMONA Research Simulator discussed in this paper. This research was supported by the Technology Foundation STW, the applied Science Division of The Netherlands Organization for Scientific Research (NWO), and the Technology Program of the Ministry of Economic Affairs.

## References

[1] Stapleford, R. L., Peters, R. A., and Alex, F. R., "Experiments and a Model for Pilot Dynamics with Visual and Motion Inputs," Systems Technology, Inc. NASA-CR-1325, Hawthorne, CA, 1969.

[2] Hosman, R. J. A. W., "Pilot's Perception and Control of Aircraft Motions," Ph.D. Thesis, Faculty of Aerospace Engineering, Delft University of Technology, Delft, The Netherlands, 1996.

[3] van der Vaart, J. C., "Modelling of Perception and Action in Compensatory Manual Control Tasks," Ph.D. thesis, Faculty of Aerospace Engineering, Delft University of Technology, 1992.

[4] Pool, D. M., Mulder, M., Van Paassen, M. M., and van der Vaart, J. C., "Effects of Peripheral Visual and Physical Motion Cues in Roll-Axis Tracking Tasks," *Journal of Guidance, Control, and Dynamics*, Vol. 31, No. 6, 2008, pp. 1608–1622. doi:10.2514/1.36334

[5] Zacharias, G. L., and Young, L. R., "Influence of Combined Visual and Vestibular Cues on Human Perception and Control of Horizontal Rotation," *Experimental Brain Research*, Vol. 41, No. 4, Jan. 1981, pp. 159–171. doi: 10.1007/BF00236605

[6] Schroeder, J. A., "Helicopter Flight Simulation Motion Platform Requirements," NASA Ames Research Center TP-1999-208766, Moffett Field, CA, 1999.

[7] Grant, P. R., Yam, B., Hosman, R. J. A. W., and Schroeder, J. A., "Effect of Simulator Motion on Pilot Behavior and Perception," *Journal of Aircraft*, Vol. 43, No. 6, 2006, pp. 1914–1924. doi:10.2514/1.21900

[8] Ellerbroek, J., Stroosma, O., Mulder, M., and Van Paassen, M. M., "Identification of the Roles of Yaw and Sway Motion in Helicopter Yaw Control Tasks," *Journal of Aircraft*, Vol. 45, No. 4, 2008, pp. 1275–1289.

[9] van Gool, M. F. C., and Mooij, H. A., "A Comparison of In-Flight and Ground-Based Pitch Attitude Tracking Experiments," *Proceedings of the 12th Annual Conference on Manual Control*, NASA Ames Research Center, Moffett Field, CA, 1976, pp. 443–454.

[10] Steurs, M., Mulder, M., and van Paassen, M. M., "A Cybernetic Approach to Assess Flight Simulator Fidelity," AIAA Paper 2004-5442, 2004.

[11] Dehouck, T. L., Mulder, M., and van Paassen, M. M., "The Effects of Simulator Motion Filter Settings on Pilot Manual Control Behaviour," AIAA Paper 2006-6250, 2006.

[12] van den Berg, P., Zaal, P. M. T., Mulder, M., and van Paassen, M. M., "Conducting Multi-Modal Pilot Model Identification—Results of a Simulator Experiment," AIAA Paper 2007-6892, 2007.

[13] Groot, T., Damveld, H. J., Mulder, M., and Van Paassen, M. M., "Effects of Aeroelasticity on the Pilot's Psychomotor Behavior," AIAA Paper 2006-6494, 2006.

[14] McRuer, D. T., Graham, D., Krendel, E., and Reisener, W., "Human Pilot Dynamics in Compensatory Systems. Theory, Models and ExperimentsWith Controlled Element and Forcing Function Variations," Systems Technology, Inc., and the Franklin Inst. AFFDL-TR-65-16, 1965.

[15] Nieuwenhuizen, F. M., Zaal, P. M. T., Mulder, M., van Paassen, M. M., and Mulder, J. A., "Modeling Human Multi-Channel Motion Perception and Control Using Linear Time-Invariant Models," *Journal of Guidance, Control, and Dynamics*, Vol. 31, No. 4, 2008, pp. 999–1013. doi:10.2514/1.32307

[16] van der Linden, C. A. A. M., "DASMAT—Delft University Aircraft Simulation Model and Analysis Tool: A Matlab/Simulink Environment for Flight Dynamics and Control Analysis," Delft University of Technology, Faculty of Aerospace Engineering Rept. LR-781, 1996, ISBN 90-5623-053-0.

[17] Levison, W. H., "A Model for the Pilot's Use of Roll-Axis Motion Cues in Steady-State Tracking Tasks," Bolt Beranek and Newman, Inc. Tech. Rept. 3808, 1978.

[18] Zaal, P. M. T., Nieuwenhuizen, F. M., Mulder, M., and Van Paassen, M. M., "Perception of Visual and Motion Cues During Control of Self-Motion in Optic Flow Environments," AIAA Paper 2006-6627, Aug. 2006.

[19] Berkouwer, W. R., Stroosma, O., van Paassen, M. M., Mulder, M., and Mulder, J. A., "Measuring the Performance of the SIMONA Research Simulator's Motion System," AIAA Paper 2005-6504, Aug. 2005.

[20] Reid, L. D., and Nahon, M. A., "Flight Simulation Motion-Base Drive Algorithms. Part 1: Developing and Testing the Equations," University of Toronto, Institute for Aerospace Studies Rept. 296, 1985.

[21] De Bruin, J., Mulder, M., Van Paassen, M. M., Zaal, P. M. T., and Grant, P. R., "Pilot's Use of Heave Cues in a Pitch Control Task," AIAA Paper 2007-6895, 2007.

[22] McRuer, D. T., and Krendel, E. S., "AGARD Advisory Report No. 188: Mathematical Models of Human Pilot Behavior," AGARD Rept. AG-144, 1974.

[23] Jex, H. R., Magdaleno, R. E., and Junker, A. M., "Roll Tracking Effects of G-Vector Tilt and Various Types of Motion Washout," *Proceedings of the 14th Annual Conference on Manual Control*, NASA Ames Research Center, Moffett Field, CA, 1978, pp. 463–502.

[24] McRuer, D. T., and Jex, H. R., "A Review of Quasi-Linear Pilot Models," *IEEE Transactions on Human Factors in Electronics*, Vol. HFE-8, No. 3, 1967, pp. 231–249. doi:10.1109/THFE.1967.234304